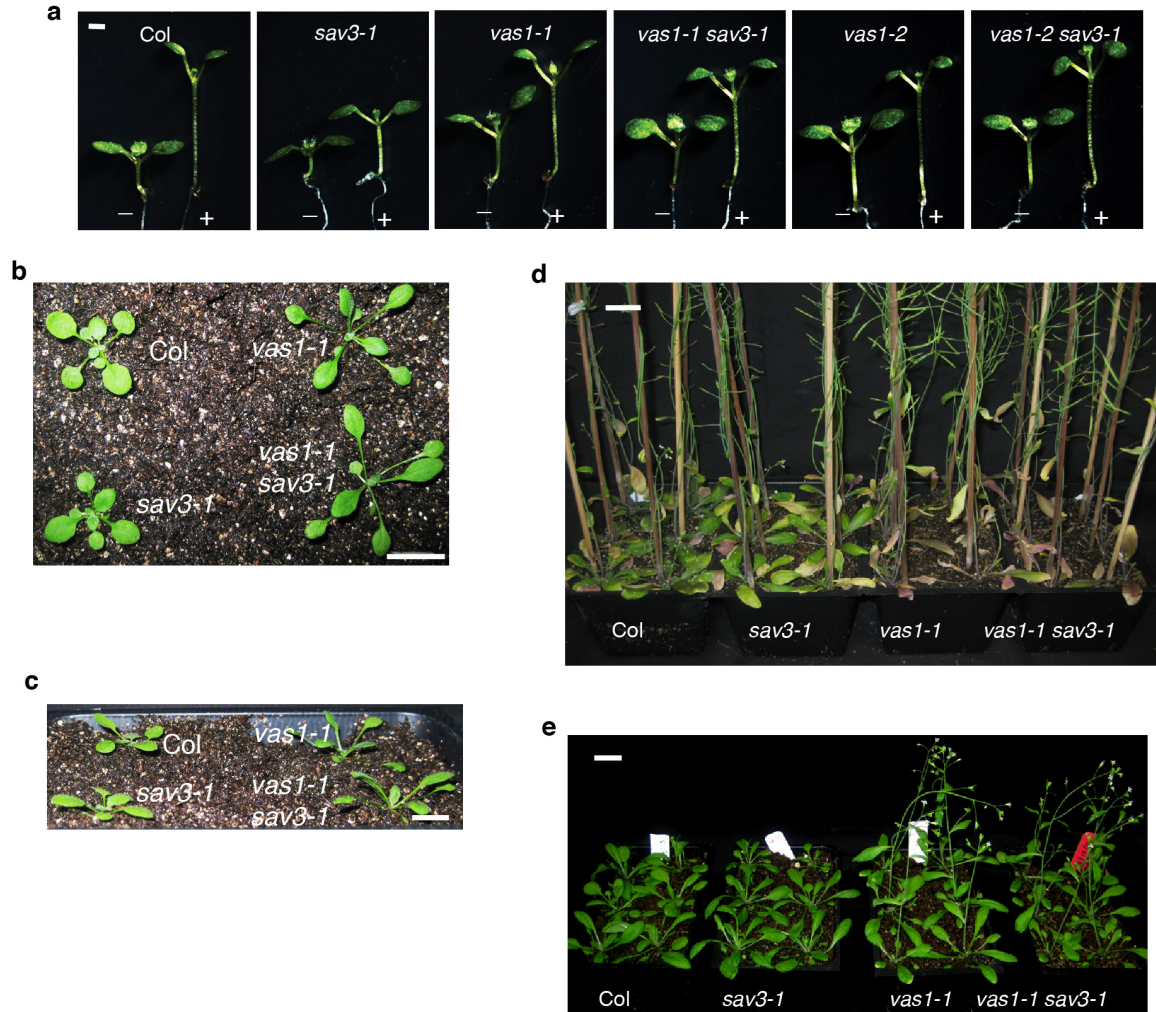


SUPPLEMENTARY INFORMATION

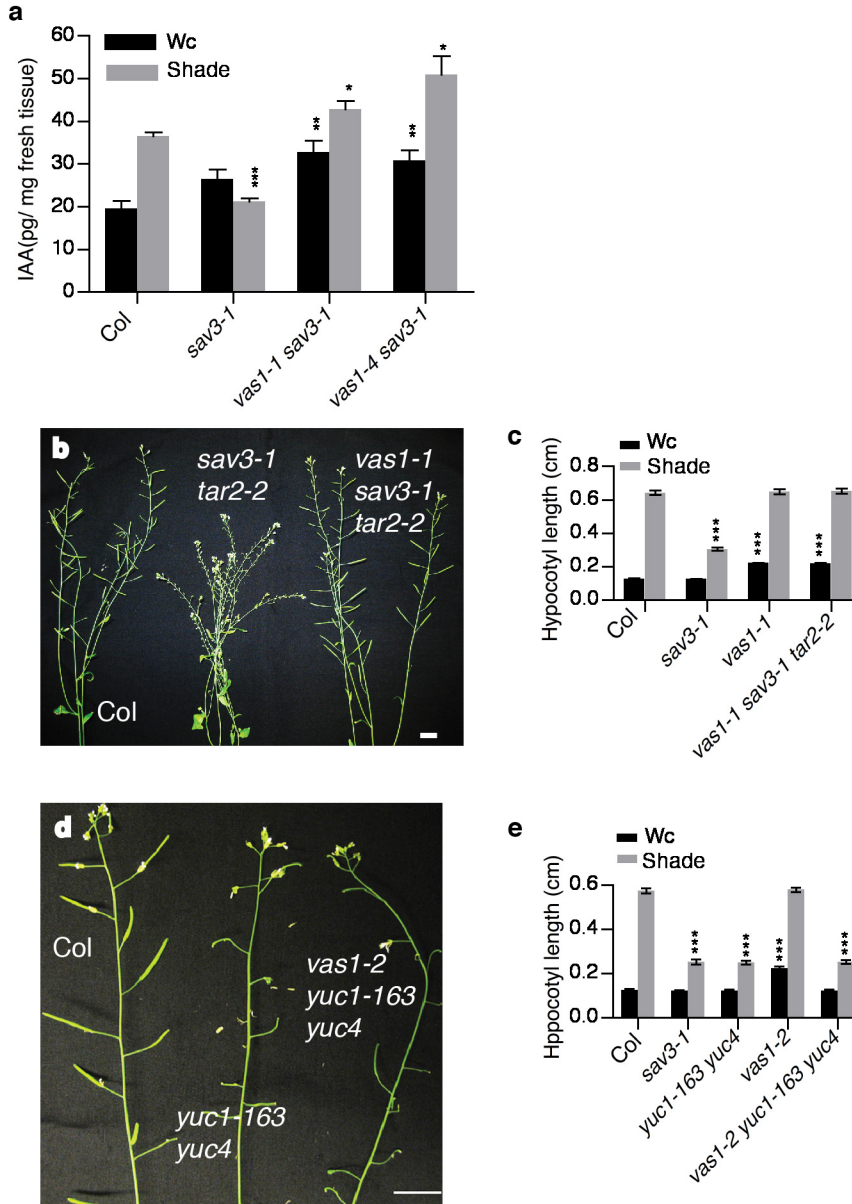
**Coordination of auxin and ethylene biosynthesis by the
aminotransferase VAS1**

Zuyu Zheng, Yongxia Guo, Ondřej Novák, Xinhua Dai, Yunde Zhao, Karin Ljung, Joseph
P. Noel & Joanne Chory

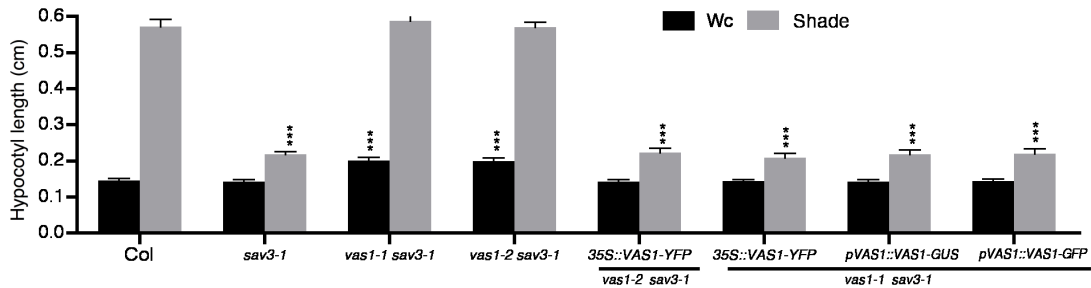
SUPPLEMENTARY RESULTS

**Supplementary Figure 1. Mild constitutive SAS of *vas1-1* and *vas1-1 sav3-1* mutants.**

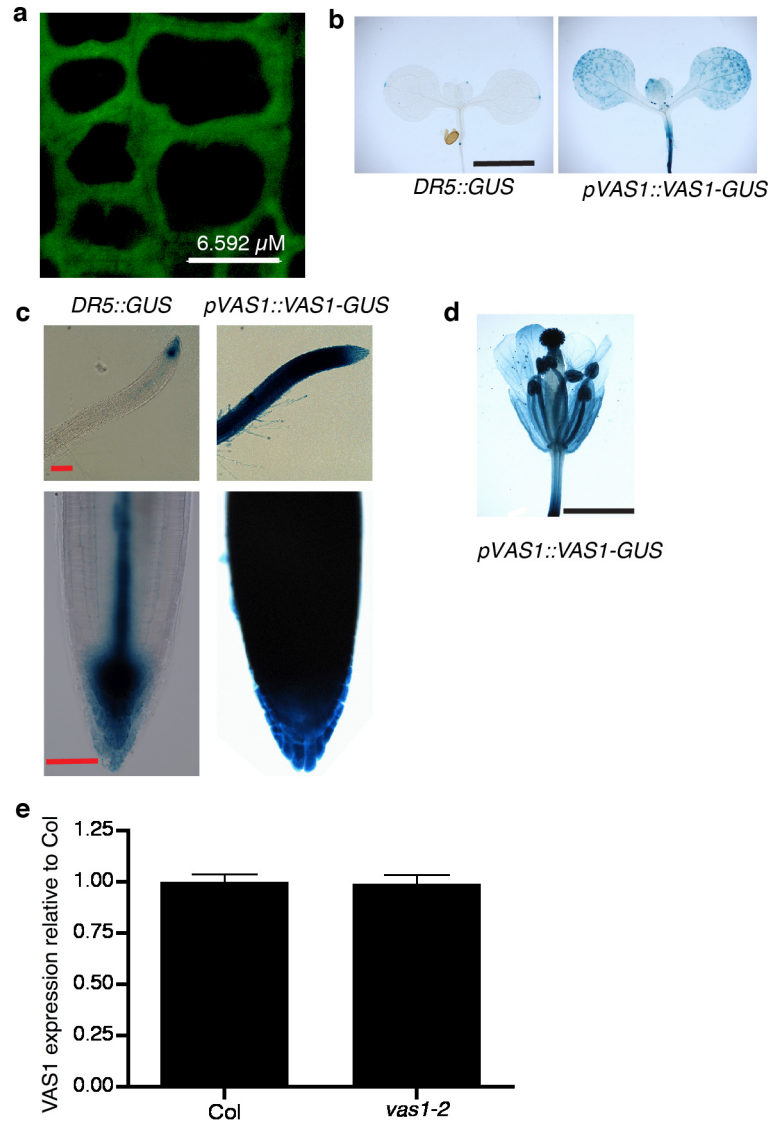
a, *vas1* rescued the *sav3* hypocotyl elongation defect in response to shade. The plants were grown on $\frac{1}{2}$ MS plates, and kept under white light (Wc) for 5 d and then remained in Wc for 4 d (-) or transferred to shade for 4 d (+). Scale bar 1 mm. **b and c**, *vas1-1* and *vas1-1 sav3-1* plants had increased petiole length (**b**) and increased leaf hyponasty (**c**). Images of 18 d old Col-0, *sav3-1*, *vas1-1 sav3-1*, and *vas1-1* plants grown in a long-day growth room were shown. Scale bar 1 cm. **d**, *vas1-1* and *vas1-1 sav3-1* mutants displayed accelerated leaf senescence. The plants were grown in a long-day growth room. Scale bar 2 cm. **e**, *vas1-1* and *vas1-1 sav3-1* plants flowered earlier compared with Col-0 and *sav3-1*. Image of 40 day old Col-0, *sav3-1*, *vas1-1 sav3-1*, and *vas1-1* plants grown in a long-day growth room were shown. Scale bar 2 cm.



Supplementary Figure 2. VAS1 functioned in auxin metabolism, downstream of TAA1/SAV3 but upstream of YUCs. **a**, *vas1 sav3* accumulated higher levels of IAA in both Wc and shade ($n=3$). **b**, *vas1* rescued the fertility defect of *sav3-1 tar2-2* double mutant. Image of 50 day old plants grown in a long-day growth room were shown. Scale bar 1 cm. **c**, *vas1-1 sav3-1 tar2-2* triple mutants had longer hypocotyls than *sav3-1* mutants ($n=15$). **d**, *vas1-2* failed to rescue the fertility defect of *yuc1-163 yuc4* mutant. Scale bar 1 cm. **e**, Hypocotyl elongation of *vas1-2* was compromised by *yuc1-163 yuc4* mutations ($n=15$). Results were shown as means \pm s.e.m., * $P < 0.05$, ** $P < 0.01$, and *** $P < 0.001$ (two-tailed Student's *t*-test). The comparison was made between WT Col plants and mutants under the same growth conditions and same treatment.

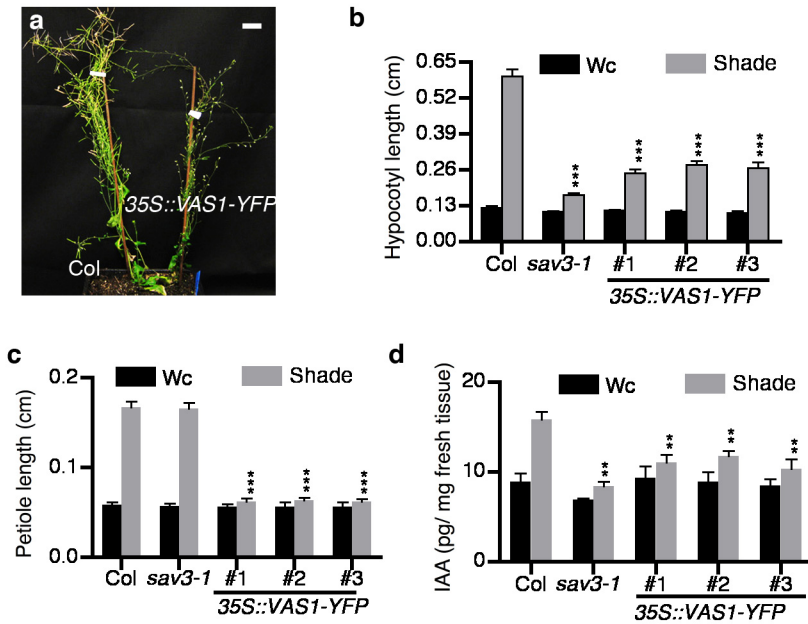


Supplementary Figure 3. Complementation experiments of the *vas1-1 sav3-1* and *vas1-2 sav3-1* double mutant. The *35S::VAS1-YFP*, *pVAS1::VAS1-GFP* or *pVAS1::VAS1-GUS* constructs were transformed into the *vas1-1 sav3-1* (or *vas1-2 sav3-1*) double mutant plants (n=15). Values were means \pm s.e.m., *** $P < 0.001$ (two-tailed Student's *t*-test). The comparison was made between WT Col plants and mutants or transgenic lines under identical growth condition.

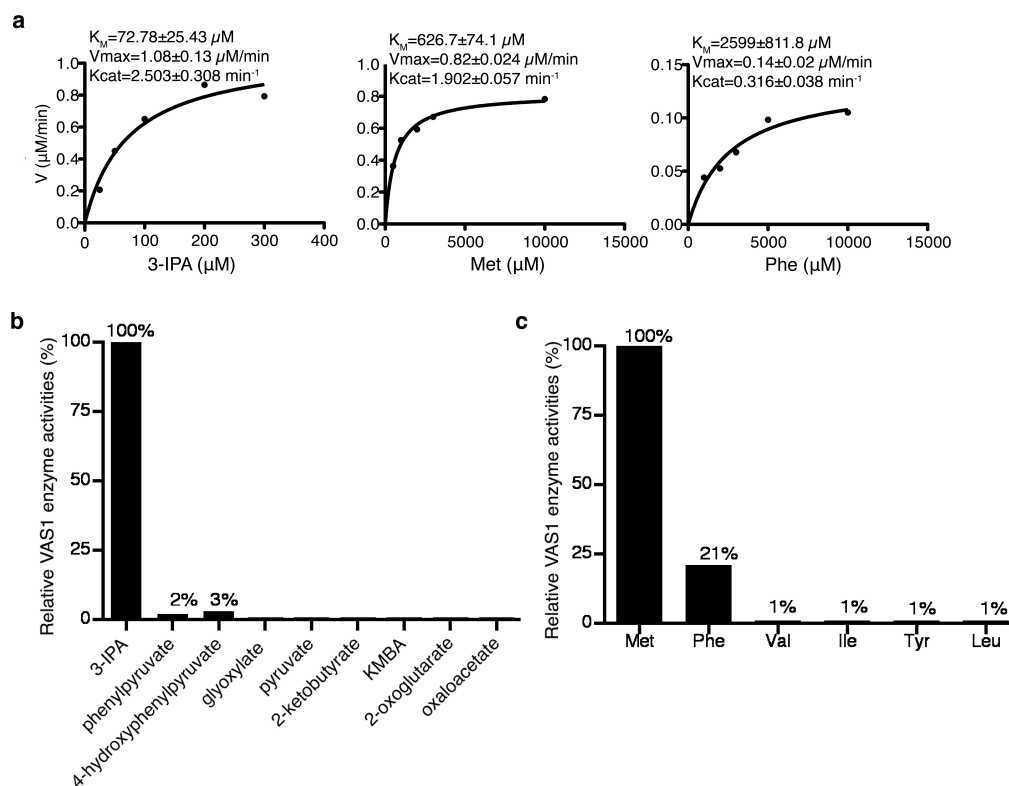


Supplementary Figure 4. Cytoplasmic localization and expression patterns of VAS1.

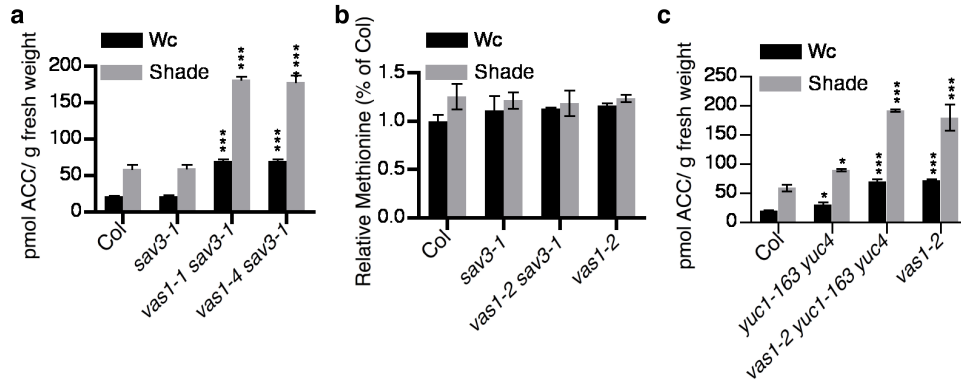
a, Cytoplasmic localization of VAS1-GFP protein in root tips. *pVAS1::VAS1-GFP* transgenic lines were generated and the VAS1-GFP fusion protein was visualized by a Leica confocal microscope. **b**, Expression patterns *pVAS1::VAS1-GUS* reporter gene in shoot. *DR5-GUS* reporter gene was included. Scale bar 2 mm. **c**, Strong expression of *pVAS1::VAS1-GUS* reporter genes in roots. *DR5-GUS* reporter gene was included. Scale bar 0.1 mm (upper panel); 50 μm (lower panel). **d**, Expression patterns of *pVAS1::VAS1-GUS* reporter gene in flowers. Scale bar 2 mm. The GUS staining were stained for 3 hrs (**b** and **c**) or 6 hrs (**d**) at 37°C in the dark. **e**, VAS1 mRNA levels were not affected by *vas1-2* mutation. VAS1 expression was quantified by real time RT-PCR. The transcript abundances of VAS1 were normalized to those of the reference gene (*At2g39960*); the data relative to those of WT were shown. Values were means \pm s.e.m., and no significant difference was observed by two-tailed Student's *t*-test using 0.05 cut-off.



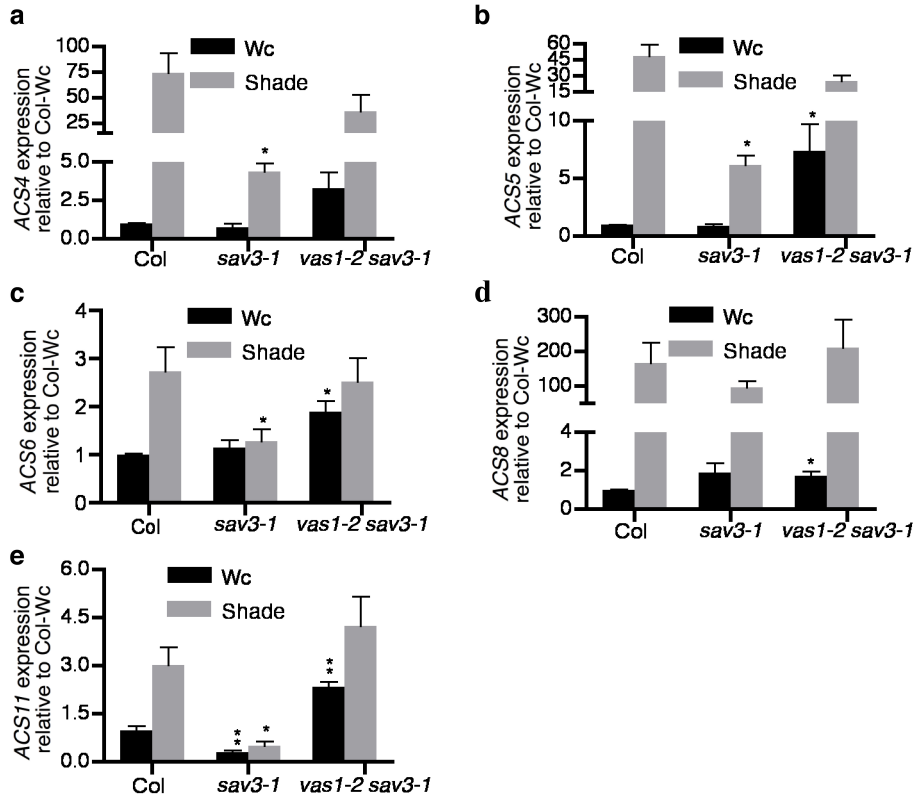
Supplementary Figure 5. Phenotypes of *35S::VAS1-YFP* transgenic lines. **a**, Constitutive overexpression of *VAS1-YFP* in wild-type Col plants (*35S::VAS1-YFP*) resulted in reduced fertility. Scale bar 2 cm. **b**, *35S::VAS1-YFP* transgenic lines showed defect in shade-induced hypocotyl elongation (n=15). Three independent transgenic lines of *35S::VAS1-YFP* in the Col-0 background are shown. **c**, *35S::VAS1-YFP* transgenic lines showed defect in shade-induced petiole elongation (n=12). **d**, *35S::VAS1-YFP* transgenic lines had lower auxin levels than WT in response to shade (n=4). Three independent transgenic lines of *35S::VAS1-YFP* in the Col-0 background were shown. Results in **b** and **c** were shown as means \pm s.e.m., $**P < 0.01$, and $***P < 0.001$ (two-tailed Student's *t*-test). The comparison was made between WT Col plants and mutants under identical growth condition.



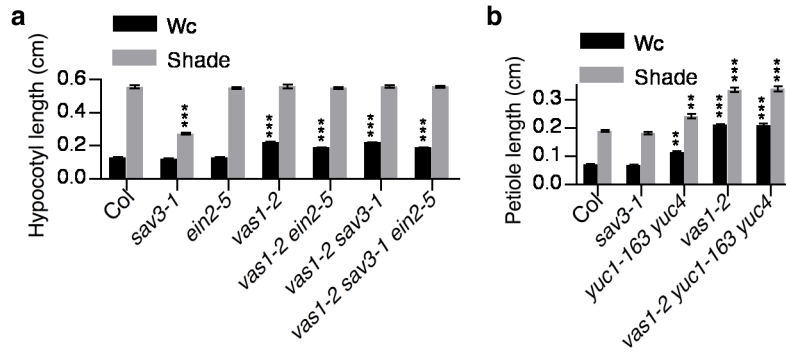
Supplementary Figure 6. Analysis of VAS1 enzyme activities. **a**, Steady-state kinetic analyses of VAS1. Curves were fit to the Michaelis-Menten equation and were displayed from left to right. Left curve: fixed concentration of L-Met (10 mM) and variable concentrations of 3-IPA from 25 to 300 μM . Middle curve: fixed concentration of 3-IPA (300 μM) and variable concentrations of L-Met from 0.5 to 10 mM. Right curve: fixed concentration of 3-IPA (300 μM) and variable concentrations of L-Phe from 1 to 10 mM. Apparent K_M , V_{max} and k_{cat} of VAS1 were shown above each curve and standard errors calculated from Graphpad Prism 5 software (www.graphpad.com). **b**, 3-IPA was the most suitable amino acceptor in the VAS1 catalyzed transamination reaction. The ketoacids, including glyoxylate, pyruvate, 2-ketobutyrate, KMBA, 2-oxoglutarate, and oxaloacetate, could not function as the amino acceptors in the VAS1 catalyzed transamination reaction. **c**, Met was the most suitable co-substrate in the VAS1 catalyzed transamination reaction. We tested VAS1 activities with 19 different amino acids as potential *in vitro* co-substrates of 3-IPA in VAS1 catalyzed transamination reactions. The results demonstrated that Met was the most suitable amino donor; the relative activity with Phe was only 21% that of Met, while Val, Ile, Tyr and Leu were 1% as active as for Met. VAS1 did not use other amino acids as amino donors.



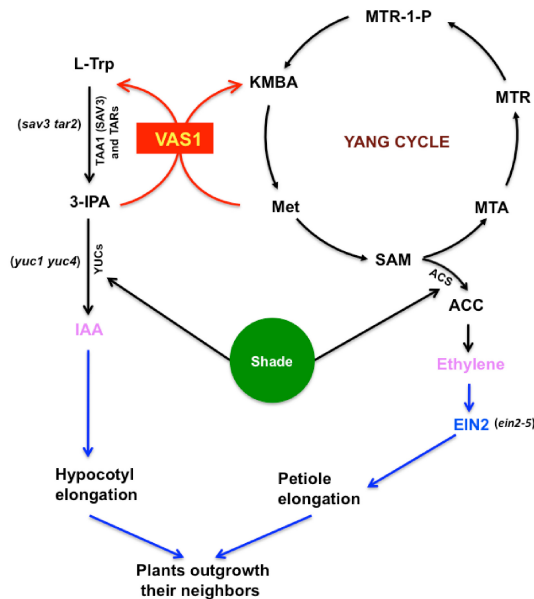
Supplementary Figure 7. Measurement of ACC levels and Met levels. **a**, *vas1-1 sav3-1* and *vas1-4 sav3-1* seedlings had increased ACC levels in both Wc and shade (n=3) compared to WT plants. **b**, Met levels in WT, *sav3-1*, *vas1-2 sav3-1* and *vas1-2* were similar (n=3). Results were shown as means \pm s.e.m., and no significant difference was observed by two-tailed Student's *t*-test using 0.05 cut-off. The comparison was made between WT Col plants and mutants under identical growth condition. **c**, Increased ACC levels in *vas1-2* were not affected by *yuc1-163 yuc4* mutations (n=3). Results were shown as means \pm s.e.m., * $P < 0.05$, ** $P < 0.01$, and *** $P < 0.001$ (two-tailed Student's *t*-test). The comparison was made between WT Col plants and mutants under same growth conditions and same treatment.



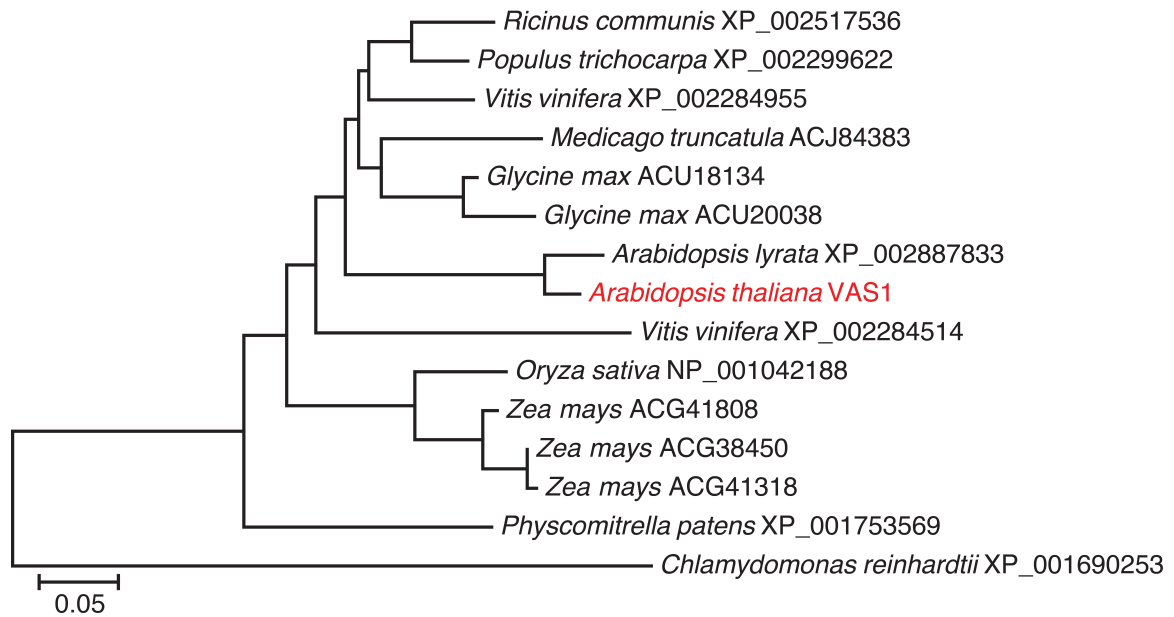
Supplementary Figure 8. The shade-induced expression of the ACS genes, including ACS4 (a), ACS5 (b), ACS6 (c), ACS8 (d) and ACS11 (e), in *vas1-2 sav3-1* was not stronger than that in WT Plants (n=3). The plants were kept in Wc or transferred to shade conditions for 1 h. The shoot part including cotyledons and hypocotyls was then collected for RNA extraction. Gene expression was quantified by real time RT-PCR. The transcript abundances of ACS genes were normalized to those of the reference gene (*At2g39960*); the data relative to those of Wc-treated WT are shown. Values were means \pm s.e.m., * $P < 0.05$ and ** $P < 0.01$ (two-tailed Student's *t*-test). The comparison was made between WT Col plants and mutants under identical growth condition.



Supplementary Figure 9. Increased ACC levels in *vas1* mutants led to exaggerated petiole elongation. **a**, The ethylene signal transduction mutation *ein2-5* did not affect *vas1-2* and *vas1-2 sav3-1* hypocotyl elongation in response to shade (n=16). **b**, Petiole elongation of *vas1-2* was not affected by *yuc1-163 yuc4* mutations (n=25). Results were shown as means \pm s.e.m., * $P < 0.05$, ** $P < 0.01$, and *** $P < 0.001$ (two-tailed Student's *t*-test). The comparison was made between WT Col plants and mutants under same growth conditions and same treatment.



Supplementary Figure 10. A model of VAS1-mediated modulation of plant shade avoidance responses through a biosynthetic hub linking auxin and ethylene biosynthesis. The VAS1 catalyzed reaction was highlighted with red lines and arrows. Shade treatment upregulates the transcription of several YUCs and ACSs, leading to biosynthesis of auxin and ethylene, respectively. The genetic and biochemical data described in this paper demonstrated that the shade-induced elongation of hypocotyls and petioles was mainly due to auxin and ethylene biosynthesis, respectively. By simultaneously slowing down the biosynthesis of auxin and ethylene, VAS1 provided an efficient metabolic mechanism to prevent plants from over-reacting to shade (R/FR=0.67).



Supplementary Figure 11. Neighbor joining tree of the VAS1 protein and VAS1-like proteins from other plant species rooted by a VAS1 homologue in the single celled green algae, *Chlamydomonas reinhardtii*.